LA-UR-74-592

CONF-740402--13

SOME NEUTRONICS ASPECTS OF LASER-FUSION REACTORS*

T. Frank, D. Dudziak, and E. Heck

University of California
Los Alamos Scientific Laboratory
Los Alamos, New Mexico

ABSTRACT

The results of initial neutronics calculations for conceptual laser-fusion power reactors are presented. Extensive calculations were done for a basic reactor model with a 4-m-diam. spherical cavity and a 1-m-thick lithium blanket region. Important neutronic characteristics were evaluated in parametric studies for other reactor sizes of interest. Niobium was assumed as the structural material; however, limited calculations were also done for systems with molybdenum structural components. The principal results include determinations of breeding ratios, energy deposition densities, primary neutron-damage effects, and induced radioactivity and afterheat.

INTRODUCTION

The pace at which laser fusion technology is developing suggest that the engineering aspects of laser-controlled power reactor systems be investigated, including the technical feasibility of several conceptual reactor cavity and blanket designs. The neutronics of these concepts have been surveyed to provide inputs leading toward detailed design specifications and to identify, as part of the iterative feedback mechanism, serious materials problems.

Many important characteristics of laser-controlled thermonuclear reactors (LCTRs) and magnetically confined thermonuclear reactors (MCTRs) are similar. Both require the breeding of tritium for the fuel cycle, the determination of energy deposition distributions, and the assessment of neutron damage effects. However, because the energy deposition in LCTRs is much faster than in MCTRs, energy deposition distributions are of particular significance in laser-fusion reactors. The energy from fusion-pellet microexplosions is deposited in fractions of a microsecond--in time intervals that are short compared to hydrodynamic time scales--which generates acoustical shock waves in the cavities and lithium blankets of these reactors. Such shock waves must be attenuated by means that depend on the energy deposition distributions. However, LCTRs offer a greater freedom in the choice of materials and in other design aspects than do most MCTRs, so that acceptable neutron-damage rates and breeding ratios seem to be attainable.

CALCULATIONAL MODEL

Most LCTR concepts being considered can be approximated reasonably well by spherical models. Accordingly, initial calculations have been restricted to such geometries. At present, only conceptual designs exist for both the reactor cavity and the blanket, and only one concept, the lithium-wetted-wall design, has been analyzed to determine structural requirements. This concept and the

---

*Work performed under the auspices of the US Atomic Energy Commission, Contract Number W-7405-ENG-36.

BLANK PAGE

analyses performed have been described elsewhere.[1] The calculational model used in the present survey was taken from the work reported earlier and is shown schematically in Fig. 1. The basic reactor model is indicated by solid lines; the dotted lines indicate a region that has been included in the model to determine the sensitivity of various neutronic responses if additional structural material is required.

The several conceptual laser-fusion reactor designs being considered are categorized according to the physical processes used to accomodate the energy deposition in the inner cavity wall.[2] These processes and the characteristics of the thermonuclear microexplosions of DT fusion pellets determine how small the reactor cavities can be. Our initial feasibility and systems studies of LCTR power plants are based on the release of 100 MJ of thermonuclear energy per pellet microexplosion, generating ~ 3.55×10^{19} fusion neutrons. The cavity diameters for 100-MJ microexplosions in most concepts are ~ 4 m, but diameters of interest may range from ~ 2 to ~ 10 m. Extensive calculations were done for the basic reactor model (referred to as a point design for neutronics calculations) with a cavity diameter of 4 m, not including additional structure shown by dotted lines in Fig. 1. Important neutronic characteristics were also evaluated in parametric studies for other reactor sizes of interest.

Considerable freedom apparently exists in choosing materials and dimensions for reactor cavities and blankets, which would satisfy overall requirements for structural integrity and breeding ratios of LCTR systems. Final selections will probably depend on neutron damage effects and other technical considerations. Initial neutronics calculations have been done for designs with refractory metal (i.e., niobium and molybdenum) structures and liquid lithium blankets. Region compositions and dimensions used for the point design are given in Table I.

CALCULATIONAL TECHNIQUES

Calculations were done of neutron and γ-ray spectral and spatial distributions, tritium production, energy deposition, various neutron damage primary effects, activation levels, and afterheat. The DTF-IV discrete ordinates code[3] was used in the S_4-P_3 approximation with 100 energy-group cross sections for neutronics calculations, and in the S_8-P_3 approximation with 21 energy-group cross sections for calculation of secondary γ-ray distributions. A point source of neutrons with an energy spectrum corresponding to fusion neutrons from DT reactions was included at the center of the calculational model. The moderating effect of fusion-pellet constituents on the source neutron energy spectrum is negligible. Neutron and γ-ray multigroup cross-section data were processed[4] from existing ENDF/B files. Calculations of energy deposition utilized kerma factors from Ref. 5, although recent data[6] more consistent with ENDF/B (i.e., in conserving energy) will be used in the next iteration of systems studies. Response functions for displacements per atom were those of Doran and Kulcinski,[7] which also will be updated in future system studies by incorporating a recent secondary displacement model.[8,9] Other response functions such as activation and transmutation cross sections were taken from the LASL/CTR multigroup library.[4]

TRITIUM PRODUCTION AND ENERGY DEPOSITION

The only materials degrading the neutron spectrum are lithium and niobium; thus, the neutron spectra are mainly of relatively high energy. Neutron spectra for three radial positions in the basic point design are shown in Fig. 2. The spectrum at the outer wall is also the leakage spectrum.

Tritium production and the fraction of tritium produced from ^6Li $(n,\alpha)T$ reactions is given for each region of the point design reactor in Table II. The combination of nuclear cross sections, isotopic concentrations, and neutron spectrum result in approximately equal tritium production from ^6Li and ^7Li. The fraction of tritium production from ^6Li increases from ~ 12% in the central cavity to ~ 80% in the outer blanket. The breeding ratio for the basic point design is 1.52. Introduction of the additional structural wall, as indicated in Fig. 1,

reduces the tritium breeding ratio to the range of 1.08 to 1.44. The variation in breeding ratio as a function of the position of this structure is shown in Fig. 3. There has been no attempt to maximize tritium production. Increases in breeding ratio could undoubtedly be obtained by several means, including the introduction of multiplying and moderating materials, if a tritium production facility should be desired.

The total energy deposition per original fusion neutron is 23.2 MeV for the basic point design, consisting of 16.26 MeV directly from neutron interactions, of 3.43 MeV from secondary γ-ray absorption, and of 3.52 MeV from α particles. The additional structural wall results in a decrease in energy deposition from neutron interactions and in an increase in energy deposition from secondary γ-ray absorption. The net result is a $\pm$ 5% variation in total energy deposition, depending on the radial position of the additional structure (energy deposition increases with increased radius). Energy deposition in the blanket lithium due to neutron interactions decreases by 37% if the additional structure is placed adjacent to the cavity wall, whereas the total reduction in energy deposition is only 5%. This may have important implications with regard to the generation of acoustical shocks. Energy deposition distributions from neutron interactions and from secondary γ-ray absorption are plotted versus reactor radius in Fig. 4.

Perturbations of reactor geometry were made by varying the radius of the inner cavity and holding structural component and blanket-lithium thicknesses constant. The additional structural material was placed midway between the inner cavity wall and the main pressure vessel (see Fig. 1). The dependence of breeding ratio on reactor size is shown in Fig. 5 for a range of cavity diameters from 2 to 10 m. Energy deposition from neutron interactions increases ~ 3% with increasing cavity diameter for the range considered, but decreases from secodary γ-ray absorption by about the same amount, resulting in essentially no net change.

One calculation was done to determine the effects of decreasing the lithium blanket thickness. For this case the cavity diameter was 4 m, the additional structural material was included, and the outer lithium blanket and the outer wall were removed. The breeding ratio was 1.19 and the total energy deposition per fusion neutron was 22.3 MeV--decreases of 6 and 4% respectively, from the initial design with the same cavity diameter. Removal of the lithium vapor from the central cavity results in less than 1% change in breeding ratio.

A calculation was also performed for an alternative design including the additional structural material, but with molybdenum structural components instead of niobium. Substitution of molybdenum for niobium increased the breeding ratio from 1.27 to 1.38 because of the increased (n,2n) reactions and the decreased parasitic absorption. This result could be reversed, as in the case of other CTR designs [10], if moderating materials were included.

NEUTRON PRIMARY DAMAGE EFFECTS

Neutron primary damage will be most severe for the wall surrounding the central cavity. The number of atomic displacements per atom, the amount of niobium destroyed by transmutations (98% of which was transmuted to zirconium), and the amounts of hydrogen and helium produced were calculated for the inner cavity wall for one year of operation with a pulse rate of one microexplosion per second. The results of these calculations are plotted versus cavity diameter in Fig. 6.

The neutron primary damage effects discussed above will eventually serve as the basis for determining changes in material properties which will, in turn, be used to estimate reactor component lifetimes. In the meantime, the measure of inner cavity wall lifetime for use in systems studies, as affected by neutron damage, will probably be total neutron fluence. Total neutron fluence for one year of operation with a pulse rate of one microexplosion per second is plotted versus cavity diameter in Fig. 7.

RADIOACTIVITY AND AFTERHEAT

Initial calculations were performed to estimate the severity of induced radioactivity and afterheat. Two cases were considered, the point design with a 4-m-diam. cavity and the point design with additional structural material placed midway between the cavity wall and the cavity wall and the main pressure vessel. Niobium structural components were assumed for both cases. Activation cross sections and maximum permissible concentrations (MPCS) were obtained from the LASL/CTR compilation prepared for the study reported in Ref. 11.

Calculations were made of induced radioactivity and afterheat in reactor structural components at the end of a 5 year operating period with an average neutron wall loading of 1.6 MW/m^2. The results of these calculations are given in Table III. Induced radioactivity was evaluated in terms of curies per thermal watt (Ci/W) of power generated for the isotopes resulting from activation chains initiated by neutron reactions with niobium. Biological hazard potentials, BHPs (Ci/W divided by MPC) representing the degree of dilution required for the activity produced to ensure against serious biological injury, were also determined.

Radioactivity due to ^{89}Sr and ^{90}Sr was not calculated; however, the radioactivity due to these isotopes was less than that due to ^{90}Y and ^{90m}Y both in terms of Ci/W and BHP for a design[11] with higher wall loadings than assumed in this study.

The inclusion of the additional structure increased the induced radioactivity per unit power by about a factor of two.

Afterheat is only a few tenths of one percent of the steady-state power level and appears to pose no significant problem. More detailed thermal analyses will have to be made for specific reactor components to confirm this tentative conclusion.

CONCLUSIONS

Initial neutronics calculations led to the conclusion that the freedom of choice of materials and dimensions for LCTR cavities and blankets allows the design of systems with relatively large breeding ratios and long lifetimes, insofar as neutron damage effects are concerned.

The lithium blankets that have been included in conceptual reactor designs contain more lithium than necessary to satisfy anticipated breeding-ratio requirements. Very little tritium is produced in the outer blanket region. This region could either be removed or tritium production could probably be enhanced markedly by the addition of moderating materials. Similarly, tritium breeding could be enhanced by the addition of neutron-multiplying materials (e.g., beryllium) near the cavity wall.

If it should become desirable to construct reactors for the production of tritium (say, for fueling other thermonuclear reactors in populated areas), LCTR systems could be very useful in this capacity.

Calculations of induced radioactivity and afterheat indicate that laser-fusion reactors will have biological hazard potentials and relative afterheat power densities comparable to other fusion reactors with similar cavity wall loadings.

Many additional variations of materials and geometry exist for which neutronics calculations should be performed to provide the data needed for the selection of detailed reactor and blanket designs. Among the calculations to be made are those for structures of stainless steel and sintered aluminum products (SAP), for gas-cooled blankets containing stagnant lithium, and for lithium alloys and compounds.

REFERENCES

1. Booth, L. A. (Compiler), "Central Station Power Generation by Laser-Driven Fusion," Los Alamos Scientific Laboratory Report LA-4858-MS, Vol. I, February 1972.

2. Williams, J. M.; Finch, F. T.; Frank, T. G.; and Gilbert, J. S., "Engineering Design Considerations for Laser Controlled Thermonuclear Reactors," Los Alamos Scientific Laboratory, Presented at the 5th Symposium on Engineering Problems of Fusion Research, Princeton, NJ, November 6-9, 1973.

3. Lathrop, K. D., "DTF-IV, A FORTRAN Program for Solving the Multigroup Transport Equation with Anisotropic Scattering," Los Alamos Scientific Laboratory Report LA-3373 (1965).

4. Muir, D. W., Los Alamos Scientific Laboratory, private communication.

5. Ritts, J. J.; Solomito, M.; and Steiner, D., "Kerma Factors and Secondary Gamma-Ray Sources for Some Elements of Interest in Thermonuclear Blanket Assemblies," Oak Ridge National Laboratory Report ORNL-TM-3564 (1970).

6. Abdou, M. A. and Maynard, C. W., "MACK: A Program to Calculate Neutron Energy Release Parameters and Multigroup Neutron Reactions Cross Sections from ENDF/B," Trans. Am. Nucl. Soc., 16, 129 (1973).

7. Doran, D. G. and Kulcinski, G. L., University of Wisconsin, private communication, July 1972.

8. Badger, B., et al., "UWMAK-I A Wisconsin Toroidal Fusion Reactor Design," University of Wisconsin Report UWFDM-68, V. I (1973).

9. Doran, D. G.; Beeler, J. R.; Dudey, N. D.; and Fluss, M. J., "Report of the Working Group on Displacement Models and Procedures for Damage Calculations," Hanford Engineering Development Laboratory Report HEDL-TME-73-76 (1973).

10. Dudziak, Donald J., "Nucleonic Characteristics of a Reference Theta-Pinch Reactor (RTPK) Blanket," Los Alamos Scientific Laboratory Report, to be published.

11. Dudziak, Donald J. and Krakowski, R. A., "A Comparative Analysis of D-T Fusion Reactor Radioactivity and Afterheat," Los Alamos Scientific Laboratory, Presented at First Topical Meeting on The Technology of Controlled Nuclear Fusion, San Diego, CA, April 16-18, 1974.

FIGURE CAPTIONS

1. Schematic of LCTR Calculational Model

2. Neutron spectra at various radial positions in the point reactor design.

3. Breeding ratio versus radial position of additional structural material in the point reactor design.

4. Energy deposition versus radial position in the point reactor design.

5. Breeding ratio versus reactor size.

6. Neutron damage effects in inner cavity wall for one year of operation with one fusion-pellet microexplosion per second versus cavity diameter.

7. Total neutron fluence in inner cavity wall for one year of operation with one fusion-pellet microexplosion per second versus cavity diameter.

TABLE I

VALUES USED IN LCTR CALCULATIONAL MODEL (see Fig. 1)

Region and Outer Radii, m	Material	Density, g/cm^3
Central Cavity, 1.989	Li Vapor	0.0018
Inner Cavity Wall, 2.000	60 v/o Nb	4.679
	40 v/o Li	0.224
Additional Structure (0.075 m thick)*	90 v/o Nb	7.713
	10 v/o Li	0.047
Inner Li Blanket, 2.696	Li Vapor	0.478
Main Pressure Vessel, 2.796	90 v/o Nb	7.713
	10 v/o Li	0.047
Outer Li Blanket, 3.096	Li vapor	0.472
Outer Wall, 3.121	Nb	8.570

*Radial position variable.

TABLE II

TRITIUM PRODUCTION

Region	Tritium Production, atom/source neutron	Percent of Tritium Production from ^{6}Li (n,α)T
Central cavity (Li vapor)	0.016	12.3
Inner cavity wall	0.015	33.7
Inner Li blanket	1.386	49.0
Main pressure vessel	0.007	78.8
Outer Li blanket	0.092	79.7

Breeding ratio = 1.516

TABLE III

RADIOACTIVITY AND AFTERHEAT

Operating time = 5 yr
14.1-MeV neutron wall loading = 1.6 MW/m^2

Isotope	MPC(Ci/km^3)[a]	Point Design		Point Design Plus Additional Structure[b]	
		Specific Radioactivity (Ci/W)	BHP (km^3/W)	Specific Radioactivity (Ci/W)	BHP (km^3/W)
^{92}Nb	350.0	7.14×10^{-8}	2.04×10^{-10}	1.56×10^{-7}	4.46×10^{-10}
^{92m}Nb	370.0	0.278	7.51×10^{-4}	0.606	1.64×10^{-3}
^{93m}Nb	4.0	7.96×10^{-2}	1.99×10^{-2}	0.169	4.22×10^{-2}
^{94}Nb	2.0	3.02×10^{-4}	1.51×10^{-4}	5.72×10^{-4}	2.86×10^{-4}
^{94m}Nb	2.0×10^{5}	0.886	4.43×10^{-6}	1.695	8.47×10^{-6}
^{95}Nb	3.0	6.23×10^{-2}	2.08×10^{-2}	0.174	5.81×10^{-2}
^{95m}Nb	280.0	1.247×10^{-2}	4.45×10^{-5}	3.48×10^{-2}	1.24×10^{-4}
^{90}Y	3.0	6.48×10^{-3}	2.16×10^{-3}	1.39×10^{-2}	4.65×10^{-3}
^{90m}Y	700.0	$< 6.48\times10^{-3}$	$< 9.25\times10^{-6}$	$< 1.39\times10^{-2}$	$< 1.99\times10^{-5}$
^{93}Zr	4.0	8.56×10^{-8}	2.14×10^{-8}	1.83×10^{-7}	4.56×10^{-8}
Total		1.332	0.0058	2.707	0.1070
Afterheat/Steady-State Power (%)		0.164		0.368	

[a] Donald J. Dudziak and R. A. Krakowski, "A Comparative Analysis of D-T Fusion Reactor Radioactivity and Afterheat", this Conference.

[b] Center of additional structure at 2.35m.

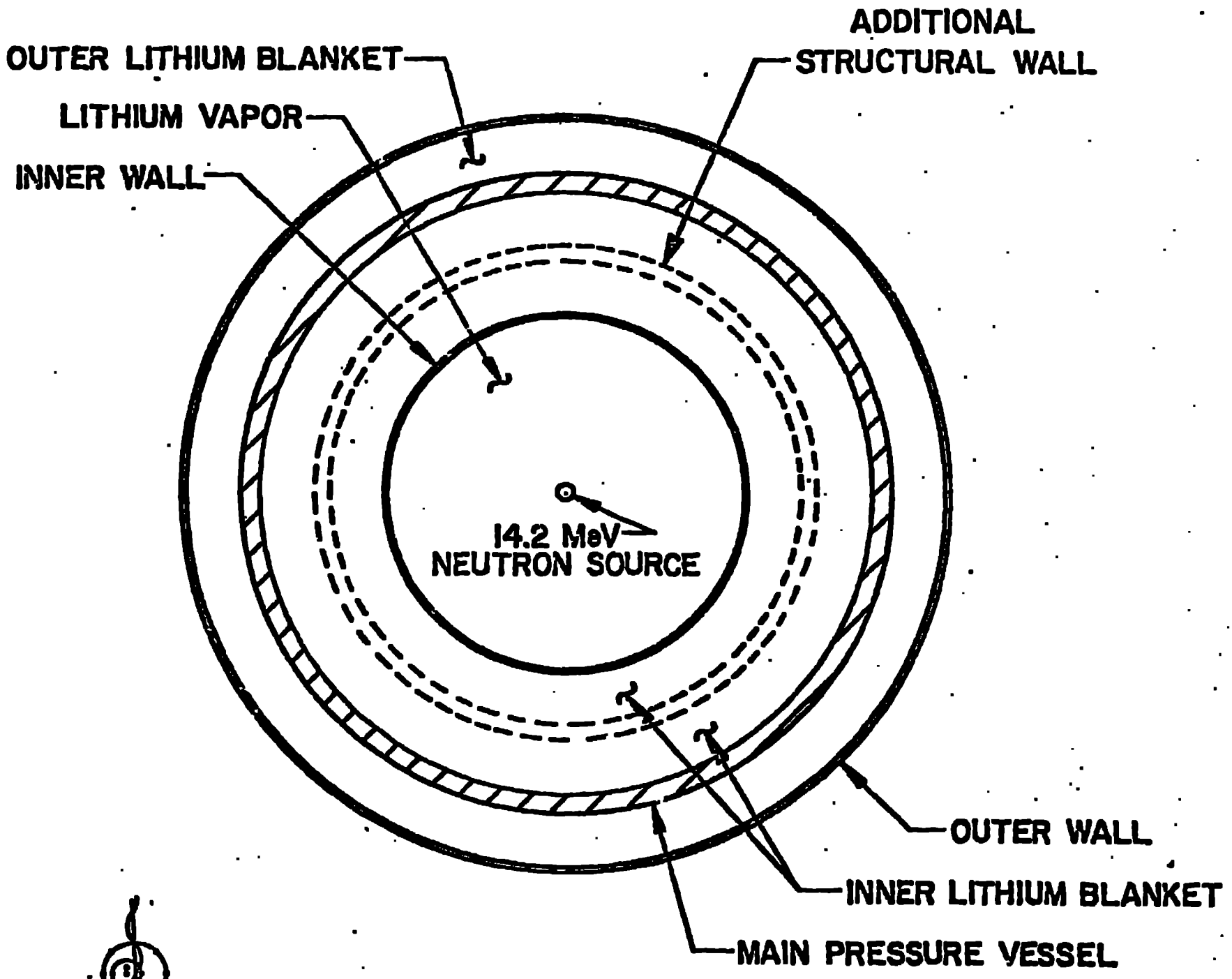

los alamos
scientific laboratory
of the University of California

LCTR calculational model

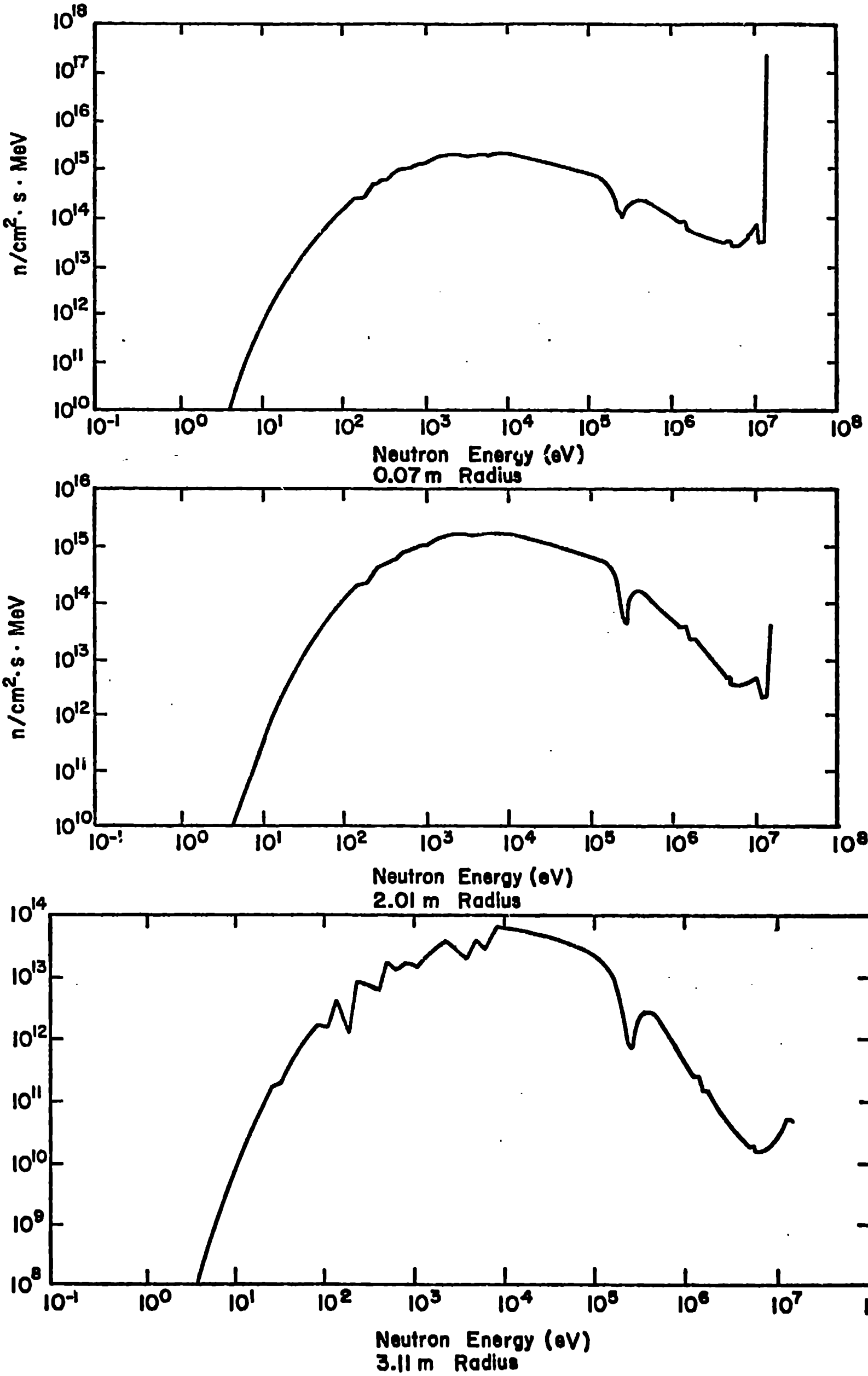
n/cm².s · MeV
10¹⁸
10¹⁷
10¹⁶
10¹⁵
10¹⁴
10¹³
10¹²
10¹¹
10¹⁰
10⁻¹
10⁰
10¹
10²
10³
10⁴
10⁵
10⁶
10⁷
10⁸
Neutron Energy (eV)
0.07 m Radius
n/cm².s · MeV
10¹⁶
10¹⁵
10¹⁴
10¹³
10¹²
10¹¹
10¹⁰
10⁻¹
10⁰
10¹
10²
10³
10⁴
10⁵
10⁶
10⁷
10⁸
Neutron Energy (eV)
2.01 m Radius
n/cm².s · MeV
10¹⁴
10¹³
10¹²
10¹¹
10¹⁰
10⁹
10⁸
10⁻¹
10⁰
10¹
10²
10³
10⁴
10⁵
10⁶
10⁷
10⁸
Neutron Energy (eV)
3.11 m Radius

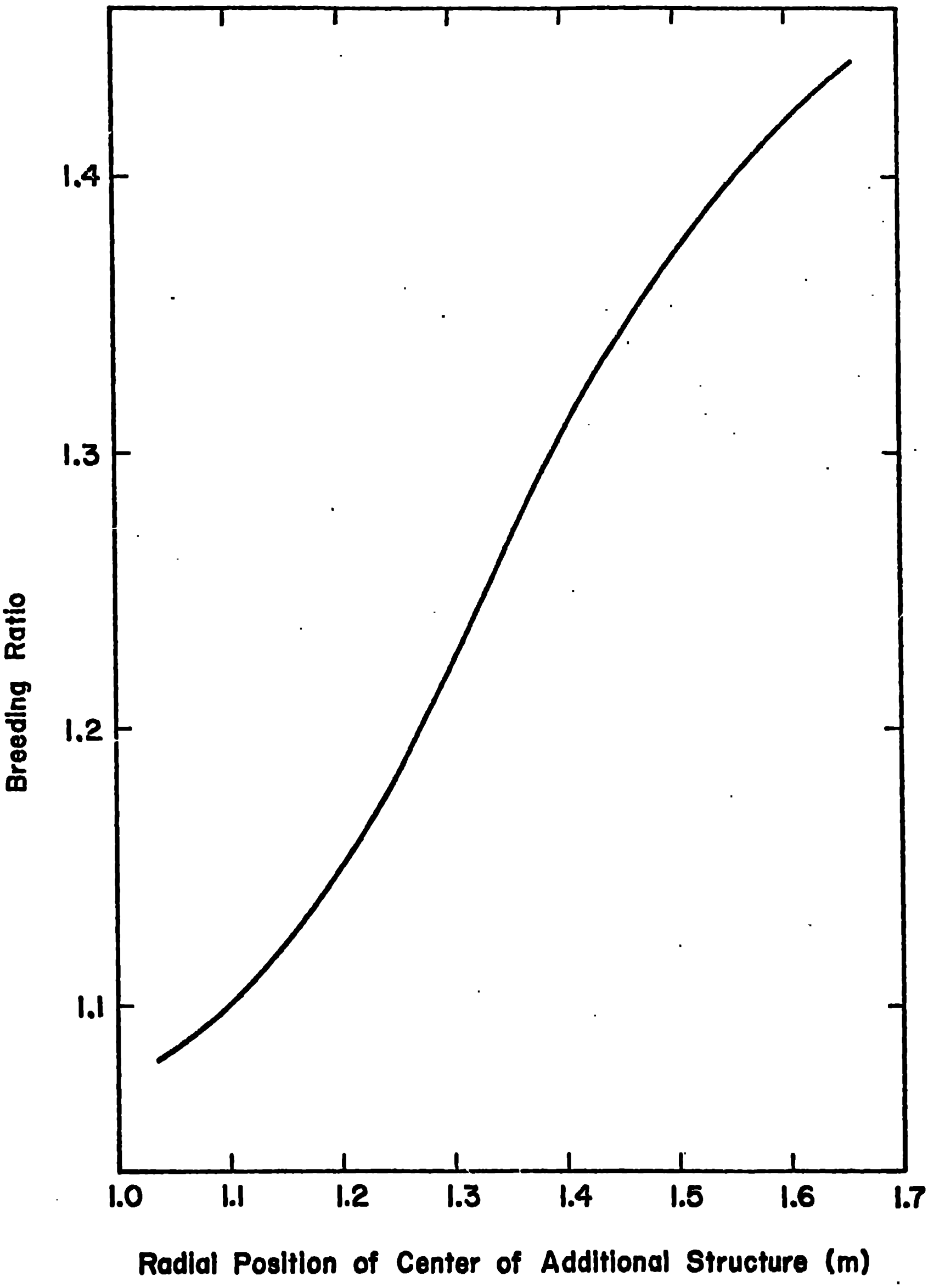
Breeding Ratio
1.4
1.3
1.2
1.1
1.0
1.1
1.2
1.3
1.4
1.5
1.6
1.7
Radial Position of Center of Additional Structure (m)

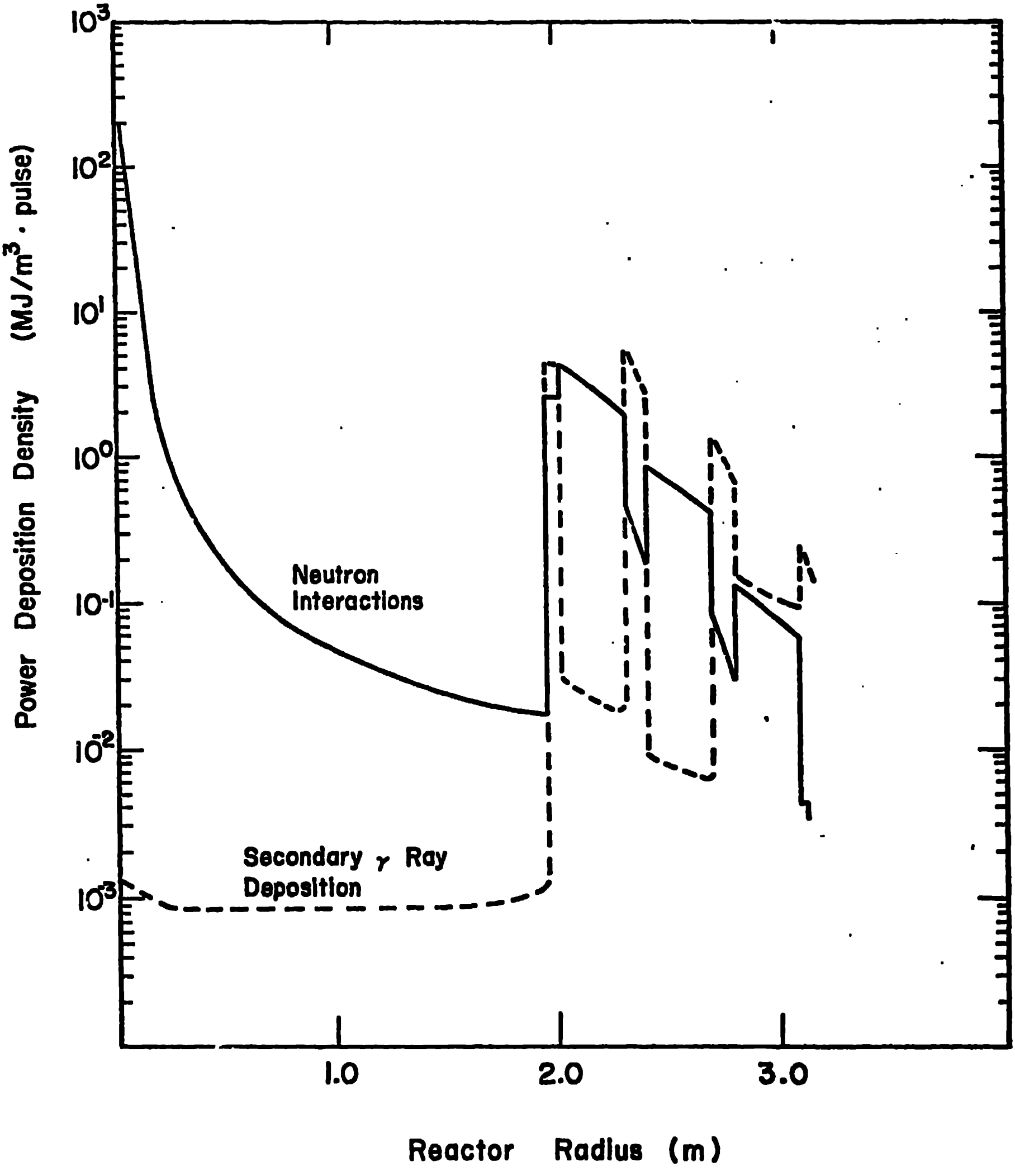
Power Deposition (MJ/m³ · pulse)
10³
10²
10¹
10⁰
10⁻¹
10⁻²
10⁻³
Neutron Interactions
Secondary γ Ray Deposition
1.0
2.0
3.0
Reactor Radius (m)

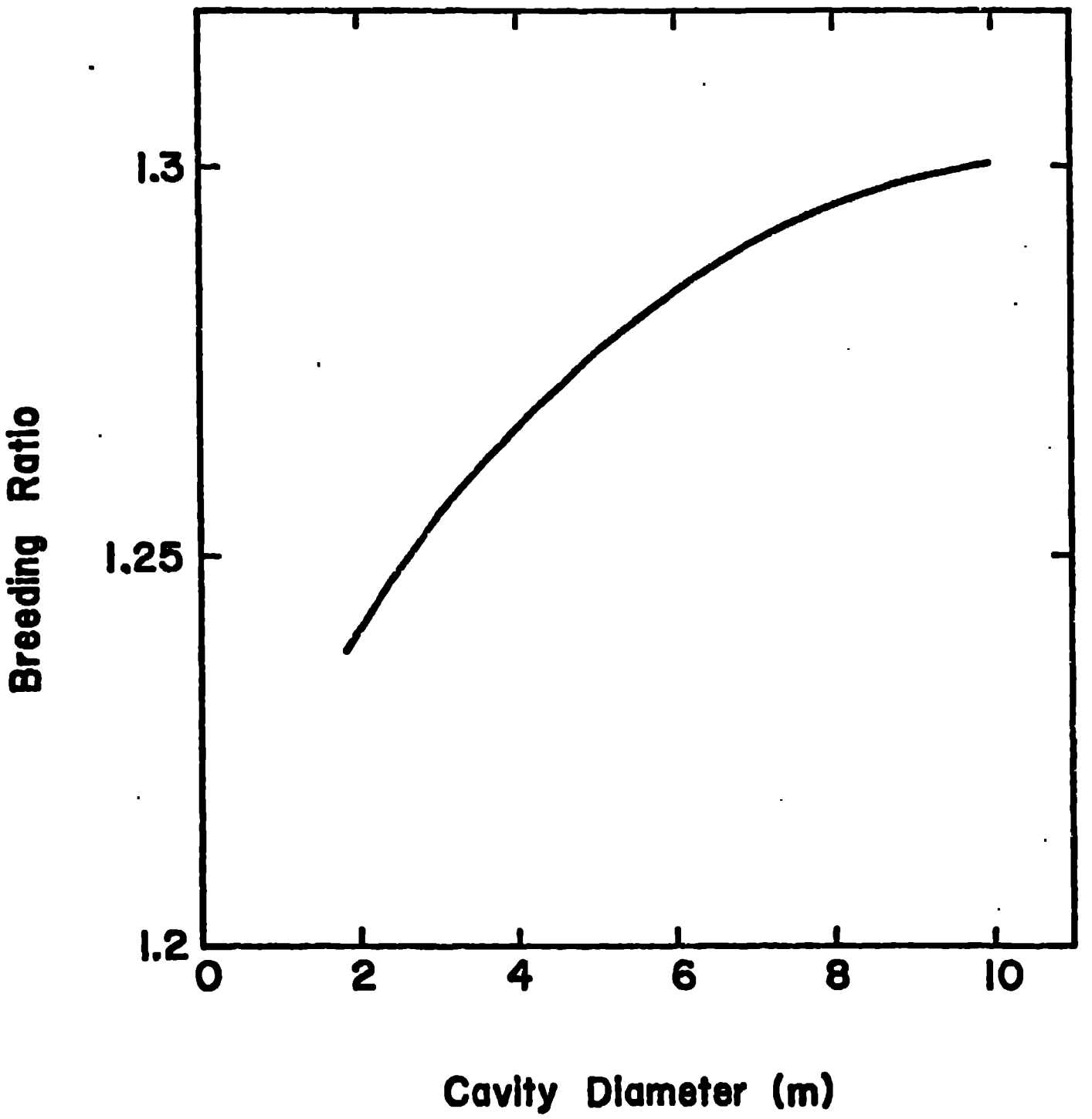
1.3
1.25
1.2
Breeding Ratio
0
2
4
6
8
10
Cavity Diameter (m)

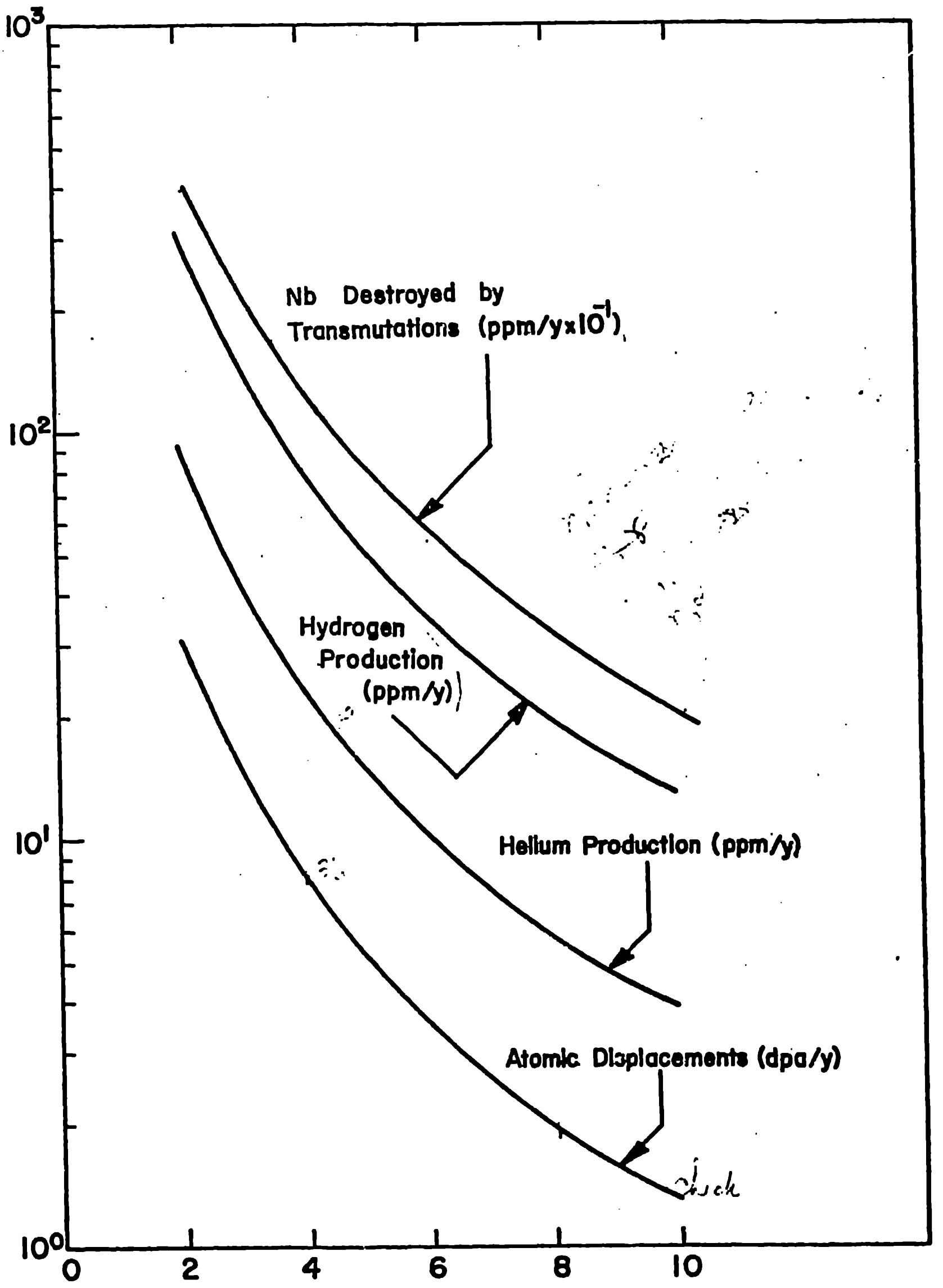
10^3
10^2
10^1
10^0
Nb Destroyed by Transmutations (ppm/y x 10^{-1})
Hydrogen Production (ppm/y)
Helium Production (ppm/y)
Atomic Displacements (dpa/y)
0
2
4
6
8
10
Cavity Diameter (m)

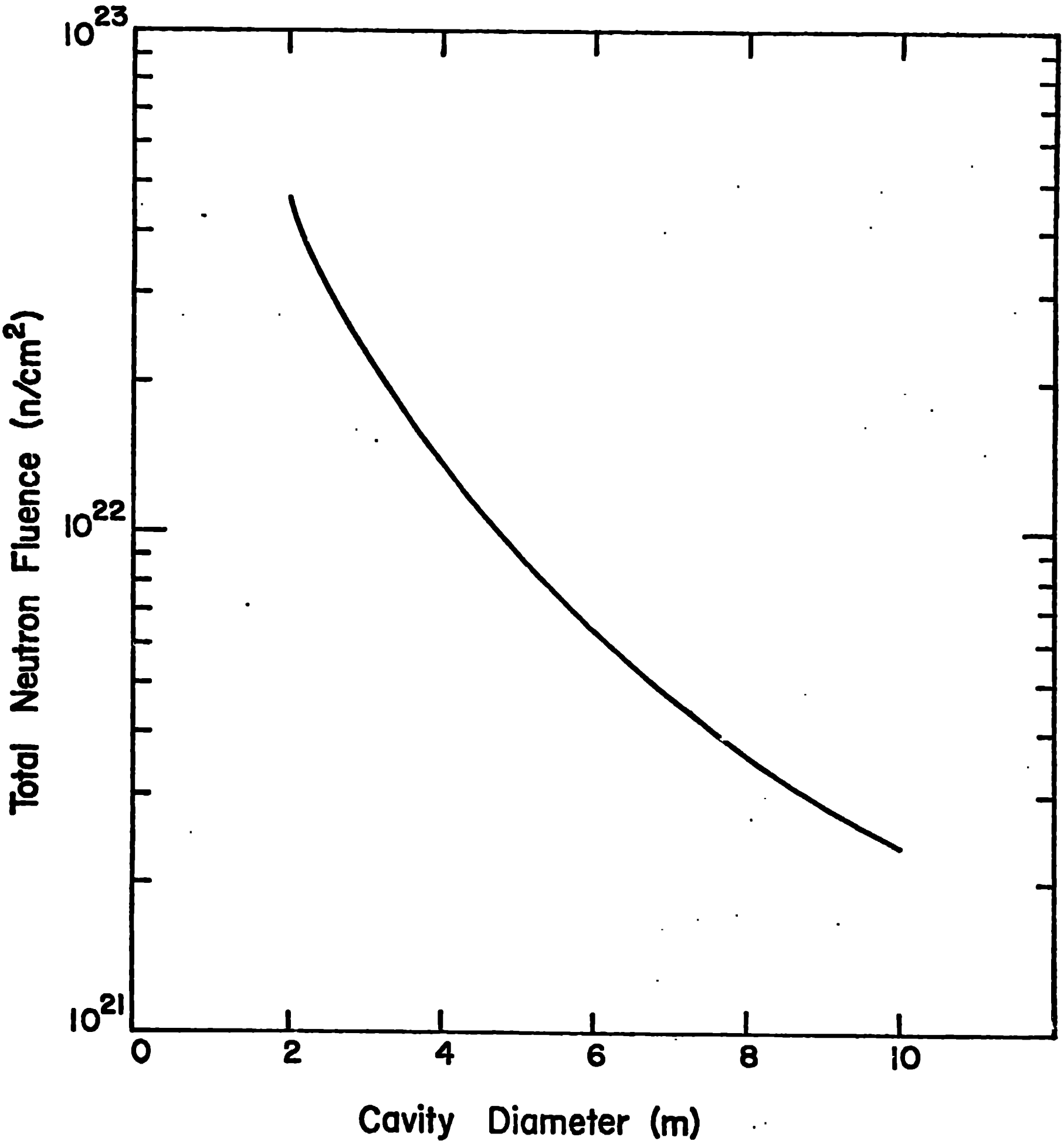
Total Neutron Fluence (n/cm²)
10²³
10²²
10²¹
0
2
4
6
8
10
Cavity Diameter (m)